Synchronous Oligocene–Miocene metamorphism of the Pamir and the north Himalaya driven by plate-scale dynamics

Michael A. Stearns[1], Bradley R. Hacker[1], Lothar Ratschbacher[2], Jeffrey Lee[3], John M. Cottle[1], and Andrew Kylander-Clark[1]
[1]Earth Science Department, University of California–Santa Barbara, Santa Barbara, California 93106, USA
[2]Geologie, Technische Universität Bergakademie Freiberg, 09599 Freiberg, Germany
[3]Geological Sciences, Central Washington University, Ellensburg, Washington 98926, USA

ABSTRACT

Gneiss domes in the Pamir (Central Asia) and the Himalaya provide key data on mid- to deep-crustal processes operating during the India-Asia collision. Laser ablation split-stream inductively coupled plasma–mass spectrometry (LASS-ICP-MS) data from monazite in these domes yield a time record from U/Th-Pb dates and a petrologic record from rare earth element (REE) abundances. Seven samples from the Pamir and six samples from the north Himalayan gneiss domes yield almost identical monazite dates of ca. 28–15 Ma. Most monazite has invariant heavy REE (HREE) abundances; two samples, however, have older monazite that records progressive HREE depletion and two samples have younger monazite that records progressive HREE enrichment. These variations in HREE are compatible with increasing garnet abundance—prograde metamorphism—until ca. 20 Ma, and decreasing garnet abundance thereafter. The change from HREE depletion to enrichment may record a transition from crustal thickening and heating to dome exhumation and cooling. This documentation of synchronous Barrovian metamorphism within domes of Indian crust along the margin of the orogen (Himalaya) and within domes of Asian crust within the core of the orogen (Pamir) is best explained by a plate-scale driving force rather than by local events. We propose that widespread, synchronous thickening was initiated by the resumption of Indian subduction following slab breakoff and then terminated by a second slab-tearing event—both plate-scale events inferred from tomography.

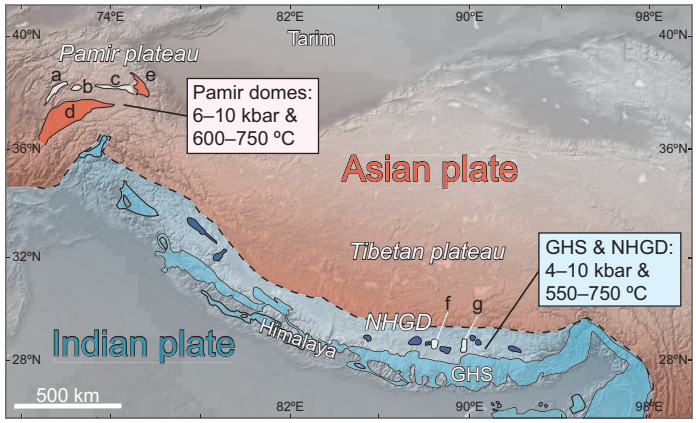

Figure 1. Geologic-topographic map, highlighting locations of north Himalayan and Pamir gneiss domes within the Cenozoic India-Asia orogen. North Himalayan gneiss domes are part of the Indian plate (blue) south of Indus-Yarlung suture, and Pamir domes formed within the Asian plate (red). Domes (those discussed in this paper are shown in white): a—Yazgulom; b—Sarez; c—Muzkol-Shatput; d—Shakhdara; e—Muztagh Ata–Kongur Shan; f—Mabja; g—Kangmar. Pressure-temperature determinations for the Pamir and the Himalaya: Greater Himalayan Series (GHS) (e.g., Simpson et al., 2000), northern Himalayan gneiss domes (NHGD) (Lee et al., 2000, 2004), and Pamir (Grew et al., 1994; Schmidt et al., 2011).

INTRODUCTION

Tectonism in orogens can be driven by local differences (e.g., in climate, rheology, rock type, crustal heterogeneities) or external boundary conditions (e.g., plate velocity). For example, changes in density distributions or thickness may give rise to buoyancy or gravitational potential energy (GPE), body forces that may drive ductile flow if they exceed rock strength. Changes in boundary forces may be linked to specific tectonic events, including crustal thickening, convective removal of lithosphere, or changes in plate dynamics (Forsyth and Uyeda, 1975).

Crustal thickening, foundering, and slab breakoff are widely invoked end-member processes occurring in orogens. Crustal thickening both directly increases and modifies GPE via phase changes. Thickening of radiogenic crust also causes temperature to increase over ~10^7 m.y. (England and Thompson, 1984), causing thermal weakening and potentially enabling flow (England and Houseman, 1989). Foundering of a gravitationally unstable portion of the lithosphere can change GPE dramatically and lead to conductive or advective heat transfer into the crust. Slab breakoff may lead to comparable changes in the upper plate as well as change trench suction, colliding resistance, or slab resistance.

The India-Asia collision (Fig. 1) affords an opportunity to examine the interplay between far-field and local causes of thickening and exhumation through examination of the middle to lower crustal chemical evolution of the orogen through time and space. Here we present new monazite petrochronology (Kylander-Clark et al., 2013, and references therein) that demonstrates that the burial and exhumation of widely separated—and apparently unrelated—crustal sections in the Pamir and the north Himalaya were synchronous, and thus best ascribed to plate-scale forces rather than local processes.

GEOLOGIC SETTING

The Himalayan front includes two arcuate belts of high-grade metamorphic and igneous rocks: the Greater Himalayan Series (GHS) and the northern Himalayan gneiss domes (NHGD; Fig. 1). These two belts contain underthrust Indian-plate schist, marble, paragneiss, and orthogneiss exhumed in the late Cenozoic (Lee and Whitehouse, 2007). Pressure-temperature-time (*P-T-t*) data indicate Barrovian metamorphism from ca. 40 Ma until 16 Ma, with crustal melting from 24 to 12 Ma (Cottle et al., 2009). Nelson et al. (1996) and others proposed that the GHS and NHGD were metamorphosed while being thrust beneath the Tibetan Plateau. The GHS was later extruded by mid-crustal flow in response to a north-south gradient in GPE, while the NHGD were exhumed by a combination of diapiric rise, transport over a thrust ramp, and upper-plate extension (e.g., Quigley et al., 2006).

In the Pamir, Barrovian metamorphic rocks and associated igneous rocks also crop out in a series of domes that were exhumed by north-south extension. Like the NHGD, the Pamir domes are built of paragneiss, schist, orthogneiss, and marble and intruded by calc-alkaline igneous rock (Schwab et al., 2004). In contrast, the domes of the Pamir crop out within the orogen interior far north of the Indus-Yarlung suture and represent crust of the Asian plate (Schwab et al., 2004). These Barrovian metamorphic rocks also experienced metamorphic conditions typical of the middle to lower crust (Fig. 1).

Thus, the eastern segment of the orogen exposes two arcuate belts of Cenozoic Indian plate–derived metamorphic rocks along the southern limit of the orogen, whereas the western segment of the orogen has Cenozoic, Asian plate–derived metamorphic domes in its interior (Fig. 1). Here we present new monazite petrochronology (Fig. 2) for the NHGD and Pamir domes to show that, in spite of these profound differences, rocks within these domes experienced peak metamorphic conditions synchronously. This finding suggests that the driving force(s) for these events were not different, local phenomenon specific to the Himalaya and the Pamir, but plate-scale dynamics capable of driving synchronous response of the entire India-Asia collision.

MONAZITE GEOCHRONOLOGY BY LASS

Monazite is an ideal phase for dating the *P-T-t*–deformation paths of metapelitic rocks because it readily reacts with major phases such as garnet, enabling one to link dates to *P-T*–dependent metamorphic reactions (e.g., Foster et al., 2000). Monazite formed at different times may have distinct chemical zones reflecting growth or recrystallization in the presence or absence of other phases (Williams et al., 1999). For example, heavy rare earth elements (HREE) and yttrium (Y) strongly partition into garnet (or xenotime), potentially enabling the use of HREE concentrations in monazite to monitor the participation of those minerals in monazite-forming reactions (Hermann and Rubatto, 2003); below we report Yb/Gd ratios as a metric of HREE depletion or enrichment.

Recent advances in laser ablation–inductively coupled plasma–mass spectrometry (LA-ICP-MS) allow more robust interpretation of dates using chemical information collected simultaneously with isotopic age data (Kylander-Clark et al., 2013). Laser ablation split-stream (LASS) ICP-MS enables determination of in situ U/Th-Pb dates and REE abundances from the same ablated material sent simultaneously to a multi-collector ICP-MS (for U/Th-Pb isotopes) and a single-collector ICP-MS (for REE).

We used LASS to measure U/Th-Pb dates (Fig. 2A) and REE concentrations (Fig. 2B; see the GSA Data Repository[1]) in monazite from seven samples from three Pamir domes, and six samples from two NHGD (Fig. 1). All the samples are pelitic to semipelitic gt + bt ± st ± ky ± sil (garnet ± biotite ± staurolite ± kyanite ± sillimanite) schists. Garnets in these samples typically have prograde zoning and are partially resorbed; a minority are neither zoned nor resorbed. Pseudosections indicate that garnet growth in these rocks was driven partly by increasing temperature and pressure (e.g., Schmidt et al., 2011). Textures indicate that monazite in most samples was produced by reaction between biotite and apatite (Bingen et al., 1996); monazite associated with staurolite may have been generated by breakdown of gt + chl (chlorite) + ms (muscovite) (Kohn and Malloy, 2004). Monazite grains exhibit several types of zoning patterns (Fig. 3; see the Data Repository): most have partially recrystallized, subhedral to anhedral low-Y cores overgrown by high-Y rims, but a minority have oscillatory zoning or are homogeneous. Different compositional zones were targeted for dating and boundaries were avoided by careful laser spot (7–10 µm) placement (Fig. 3; see the Data Repository).

The NHGD monazite dates indicate nearly continuous (re)crystallization from 29 to 14 Ma (Figs. 2A and 2B, blue data). Monazite in two Mabja dome samples shows no change in Yb/Gd from 29 to 19 Ma, whereas monazite in a third sample shows increasing depletion (decreasing Yb/Gd) from 29 to 24 Ma. Some older Mabja monazites are included in garnet, kyanite, or staurolite, whereas most of the younger dates (younger than 20 Ma) are from matrix grains. Monazite in three Kangmar dome samples ranges from 20 to 14 Ma. Two Kangmar samples exhibit no

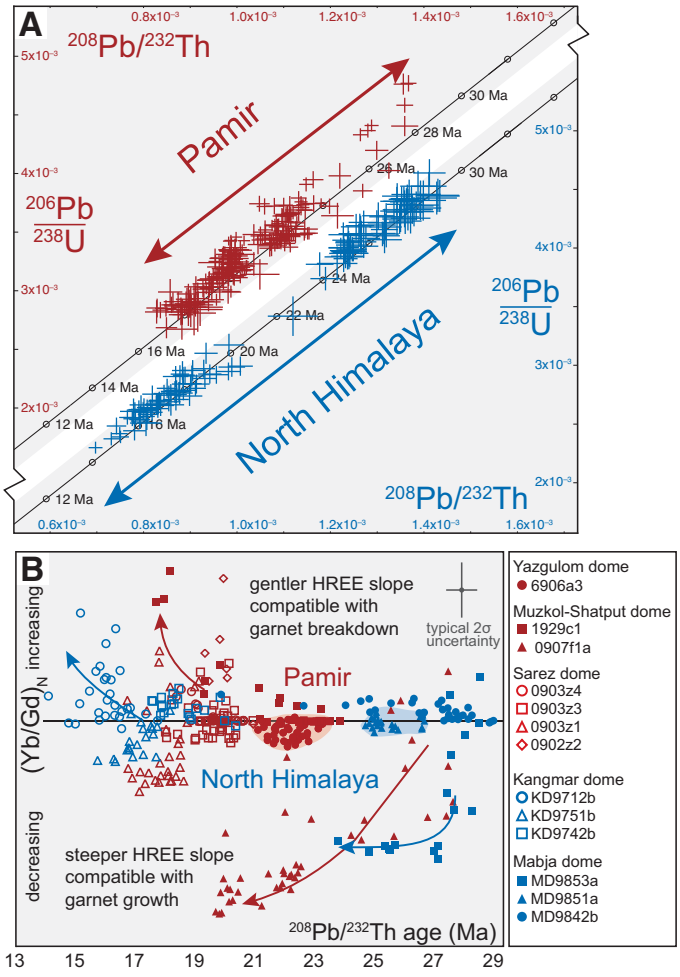

Figure 2. A: U/Th-Pb monazite dates from Pamir (red) and north Himalayan (blue) gneiss domes show similar periods of monazite (re)crystallization at ca. 28–17 Ma and ca. 29–14 Ma, respectively. B: Normalized Yb/Gd ratio versus $^{208}Pb/^{232}Th$ age. Mean Yb/Gd ratio of the five oldest spots per sample are normalized to zero to track enrichment or depletion through time. Most samples have invariant heavy rare earth element (HREE) slope. HREEs decrease over time (downward arrows) in older monazite in two samples, compatible with garnet growth. HREEs increase over time (upward arrows) in younger monazites in two other samples, compatible with garnet breakdown.

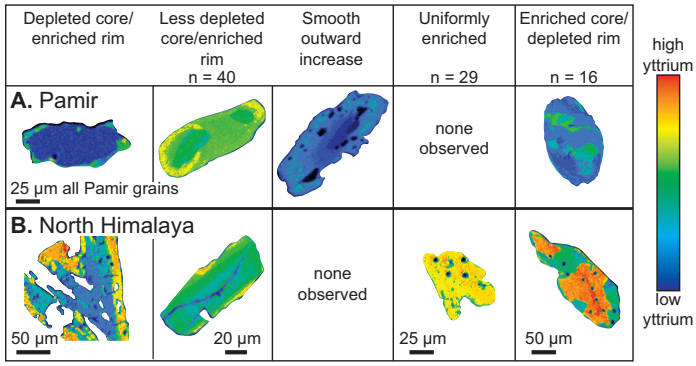

Figure 3. X-ray maps of characteristic monazites from Pamir (A) and north Himalayan (B) domes. Grains with yttrium (Y)-depleted cores and Y-enriched rims are most abundant (n = 40); oscillatory zoning or embayed cores/irregular zoning textures are less common. Y is similar in ionic radius to Ho, a heavy rare earth element (HREE) (Shannon, 1976), such that these Y maps are a proxy for HREE maps. Spots in some grains are laser holes. Total number of grains mapped is n = 85.

[1]GSA Data Repository item 2013297, Figures DR1 and DR2 (U/Th-Pb monazite concordia plots and REE spider diagrams), Figure DR3 (X-ray intensity element maps of monazite grains with analysis spots), and Table DR1 (sample descriptions and petrochronology data), is available online at www.geosociety.org/pubs/ft2013.htm, or on request from editing@geosociety.org or Documents Secretary, GSA, P.O. Box 9140, Boulder, CO 80301, USA.

change in Yb/Gd over time, whereas a third sample became progressively enriched in HREE (increasing Yb/Gd).

Monazite dates from the Pamir domes indicate growth or recrystallization from 28 to 18 Ma (Figs. 2A and 2B, red data). No sample spans the entire age range; rather, each shows a limited episode of (re)crystallization. Yazgulom dome monazite ranges from 23 to 21 Ma and has constant Yb/Gd. Monazite from the Sarez dome ranging from 21 to 17 Ma has variable Yb/Gd with no coherent pattern. Monazite in the Muzkol-Shatput dome has dates of 28–18 Ma; monazite in one sample became more depleted (decreasing Yb/Gd) from 28 to 19 Ma whereas another sample became more enriched (increasing Yb/Gd) from 24 to 17 Ma. In summary, although most Pamir monazite has invariant Yb/Gd values, samples that exhibit variation have older monazite that became progressively more depleted and younger monazite that became more enriched (Fig. 2B).

DISCUSSION

Monazite U/Th-Pb dates from the Pamir and NHGD span a nearly identical range: 28–16 Ma in the Pamir and 29–14 Ma in the NHGD (Fig. 2). Moreover, the age-related changes in monazite composition (Fig. 2B) are consistent with synchronous peak metamorphism. Older monazite in the Pamir became progressively HREE depleted from 28 to 19 Ma, and NHGD monazite (re)crystallized at this same time followed the same trend. Pamir monazite younger than 23 Ma became enriched in HREE, and NHGD monazite behaved similarly.

We interpret monazite that is HREE + Y depleted, and included within peak assemblage minerals, to record prograde metamorphism in the presence of garnet and/or xenotime (e.g., Foster et al., 2004). Some elemental zoning within monazite does not correlate with age, perhaps due to the relative immobility of REE relative to Pb (Cherniak et al., 2004). HREE depletion in monazite is compatible with increasing garnet mode or Rayleigh fractionation by phases that partition HREE, but in any case, incompatible with garnet breakdown. We interpret matrix monazite that is HREE + Y enriched to record the breakdown of garnet. HREE-enriched monazite could have crystallized from a melt, but the absence of melt textures in the central Pamir domes supports a decompression and/or cooling interpretation. This long-term pattern of monazite (re)crystallization—early HREE depletion of grains followed by younger HREE enrichment of grains—is most simply interpreted as the result of garnet growth followed by garnet breakdown. The tectonic implication is that crustal thickening produced the heating necessary for garnet growth and exhumation enabled cooling and/or decompression that drove garnet decomposition.

The matching ca. 28–15 Ma records of monazite (re)crystallization in the Pamir and Himalayan domes is surprising in light of the disparate locations and genesis of the domes: to recap, the NHGD are once-buried Indian crust at the southern margin of the orogen, and the Pamir domes are exhumed Asian crust in the center of the orogen. These new data suggest an orogen-scale process that simultaneously buried and partially exhumed both Indian and Asian crust along the margin and core of the orogen.

Synchronous Pamir and Himalaya Tectonism Driven by Plate Tectonics

The synchronous monazite (re)crystallization histories of the Pamir and Himalaya deep crust are most easily explained as the result of changes in large-scale plate dynamics (see the Data Repository). Local changes in stress state, rheology, or GPE in the Pamir and the Himalaya could only have produced synchronous changes by coincidence. Following the initial subduction of Indian continental crust at ca. 50 Ma (e.g., van Hinsbergen et al., 2011), the subducted Indian slab is inferred to have broken off on the basis of tomographic images beneath both the Pamir (Negredo et al., 2007) and Tibet (Replumaz et al., 2010), and on changes in the style and location of volcanism in Tibet (Kohn and Parkinson, 2002; Chung et al., 2003, 2005). At ca. 35 ± 5 Ma, subduction of India is inferred to have recommenced, with a buoyant lower plate forcing the upper plate to contract (Chung et al., 2003; Replumaz et al., 2010). We propose that this thickening is reflected in the ca. 28 Ma initiation of garnet-present monazite (re)crystallization in the Pamir and in the Himalaya. Monazite and zircon dates as old as ca. 39 Ma have been documented in the GHS and NHGD (Lee and Whitehouse, 2007; Cottle et al., 2009; Streule et al., 2010). Regional Barrovian metamorphism likely began at least by this time and possibly persisted for ~20 m.y. Our monazite data suggest that orogen-scale thickening then continued until ca. 20 Ma, when a second major event initiated or permitted exhumation.

It seems unlikely that the NHGD and Pamir fortuitously thickened in such a way that internal heating alone precipitated simultaneous extension. Similarly, it seems improbable that the Himalaya and the Pamir—quite different in their GPE gradients today—both reached GPE gradients conducive to north-south extension at the same time. More plausible is that the Pamir and the Himalaya were both undergoing thickening before 28 Ma and that both reached a sufficiently high GPE and a weak middle to lower crust by 20 Ma that a change in a system-wide boundary condition was able to trigger extension. That change might have been the second slab-tearing event that has been postulated—on the basis of tomography and magmatism—to have begun at ca. 25–20 Ma (Replumaz et al., 2010; DeCelles et al., 2011). We propose the monazite dates may reflect this switch, with the youngest HREE-depleted (i.e., prograde or peak metamorphic), 23–20 Ma monazite in both the Pamir and the Himalaya tracking slab tear-off and the initiation of north-south extension.

CONCLUSIONS

Monazite dates record protracted high-grade metamorphism from ca. 28–15 Ma in both the north Himalayan gneiss domes and the Pamir gneiss domes. Middle- to lower-crustal rocks in significantly different parts of the orogen experienced at least 8 m.y. of burial beginning by at least ca. 28 Ma, transitioned to exhumation by north-south crustal extension at ca. 20 Ma, and saw the end of monazite recrystallization at ca. 15 Ma. The beginning and end of Barrovian metamorphism in the Pamir and Himalayan domes relative to other significant tectonic events such as the collision of India and the transition to intra-plateau extension suggest that a common orogen-wide change in plate dynamics drove the evolution of these spatially distinct gneiss domes. This orogen-scale perspective—linking the synchronous evolution of the Pamir and north Himalayan gneiss domes—implies local processes were subordinate to larger, plate-scale processes.

ACKNOWLEDGMENTS

This project was funded by National Science Foundation grants EAR-0635485, EAR-0838146, EAR-0838269, and EAR-0923552, and DFG bundles TIPAGE (in particular RA 442/34), and CAME (subproject TIPTIMON) from the German Federal Ministry of Education and Research (support code 03G0809). Thanks to Julie Baldwin, two anonymous reviewers, and editor James Spotila.

REFERENCES CITED

Bingen, B., Demaiffe, D., and Hertogen, J., 1996, Redistribution of rare earth elements, thorium, and uranium over accessory minerals in the course of amphibolite to granulite facies metamorphism: The role of apatite and monazite in orthogneisses from southwestern Norway: Geochimica et Cosmochimica Acta, v. 60, p. 1341–1354, doi:10.1016/0016-7037(96)00006-3.

Cherniak, D.J., Watson, E.B., Grove, M., and Harrison, T.M., 2004, Pb diffusion in monazite: A combined RBS/SIMS study: Geochimica et Cosmochimica Acta, v. 68, p. 829–840, doi:10.1016/j.gca.2003.07.012.

Chung, S.L., Liu, D., Ji, J., Chu, M.F., Lee, H.Y., Wen, D.J., Lo, C.H., Lee, T.Y., Qian, Q., and Zhang, Q., 2003, Adakites from continental collision zones: Melting of thickened lower crust beneath southern Tibet: Geology, v. 31, p. 1021–1024, doi:10.1130/G19796.1.

Chung, S.L., Chu, M.F., Zhang, Y., Xie, Y., Lo, C.H., Lee, T.Y., Lan, C.Y., Li, X., Zhang, Q., and Wang, Y., 2005, Tibetan tectonic evolution inferred from spatial and temporal variations in post-collisional magmatism: Earth-Science Reviews, v. 68, p. 173–196, doi:10.1016/j.earscirev.2004.05.001.

Cottle, J.M., Searle, M.P., Horstwood, M.S.A., and Waters, D.J., 2009, Timing of midcrustal metamorphism, melting, and deformation in the Mount Everest region of southern Tibet revealed by U(-Th)-Pb geochronology: The Journal of Geology, v. 117, p. 643–664, doi:10.1086/605994.

DeCelles, P., Kapp, P., Quade, J., and Gehrels, G.E., 2011, Oligocene–Miocene Kailas basin, southwestern Tibet: Record of postcollisional upper-plate extension in the Indus-Yarlung suture zone: Geological Society of America Bulletin, v. 123, p. 1337–1362, doi:10.1130/B30258.1.

England, P., and Houseman, G., 1989, Extension during continental convergence, with application to the Tibetan Plateau: Journal of Geophysical Research, v. 94, p. 17,561–17,579, doi:10.1029/JB094iB12p17561.

England, P.C., and Thompson, A.B., 1984, Pressure-temperature-time paths of regional metamorphism I. Heat transfer during the evolution of regions of thickened continental crust: Journal of Petrology, v. 25, p. 894–928, doi:10.1093/petrology/25.4.894.

Forsyth, D., and Uyeda, S., 1975, On the relative importance of the driving forces of plate motion: Geophysical Journal of the Royal Astronomical Society, v. 43, p. 163–200, doi:10.1111/j.1365-246X.1975.tb00631.x.

Foster, G., Kinney, P., Vance, D., Prince, C., and Harris, N., 2000, The significance of monazite U-Th-Pb age data in metamorphic assemblages: A combined study of monazite and garnet chronometry: Earth and Planetary Science Letters, v. 181, p. 327–340, doi:10.1016/S0012-821X(00)00212-0.

Foster, G., Parrish, R.R., Horstwood, M.S.A., Cheney, S., Pyle, J., and Gibson, H.D., 2004, The generation of prograde P-T-t points and paths: A textural, compositional, and chronological study of metamorphic monazite: Earth and Planetary Science Letters, v. 228, p. 125–142, doi:10.1016/j.epsl.2004.09.024.

Grew, E.S., Pertsev, N.N., Yates, M.G., Christy, A.G., Marquez, N., and Chernosky, J.V., 1994, Sapphirine + forsterite and sapphirine + humite-group minerals in an ultra-magnesian lens from Kuhi-lal, SW Pamirs, Tajikistan: Are the assemblages forbidden?: Journal of Petrology, v. 35, p. 1275–1293, doi:10.1093/petrology/35.5.1275.

Hermann, J., and Rubatto, D., 2003, Relating zircon and monazite domains to garnet growth zones: Age and duration of granulite facies metamorphism in the Val Malenco lower crust: Journal of Metamorphic Petrology, v. 21, p. 833–852, doi:10.1046/j.1525-1314.2003.00484.x.

Kohn, M.J., and Malloy, M.A., 2004, Formation of monazite via prograde metamorphic reactions among common silicates: Implications for age determinations: Geochimica et Cosmochimica Acta, v. 68, p. 101–113, doi:10.1016/S0016-7037(03)00258-8.

Kohn, M.J., and Parkinson, C.D., 2002, Petrologic case for Eocene slab breakoff during the Indo-Asian collision: Geology, v. 30, p. 591–594, doi:10.1130/0091-7613(2002)030<0591:PCFESB>2.0.CO;2.

Kylander-Clark, A.R.C., Hacker, B.R., and Cottle, J.M., 2013, Laser-ablation split-stream ICP petrochronology: Chemical Geology, v. 345, p. 99–112, doi:10.1016/j.chemgeo.2013.02.019.

Lee, J., and Whitehouse, M.J., 2007, Onset of mid-crustal extensional flow in southern Tibet: Evidence from U/Pb zircon ages: Geology, v. 35, p. 45–48, doi:10.1130/G22842A.1.

Lee, J., Hacker, B.R., Dinklage, W.S., Gans, P.B., Calvert, A., Wang, Y., and Chen, W., 2000, Evolution of the Kangmar Dome, southern Tibet: Structural, petrologic, and thermochronologic constraints: Tectonics, v. 19, p. 872–895, doi:10.1029/1999TC001147.

Lee, J., Hacker, B.R., and Wang, Y., 2004, Evolution of the north Himalayan Gneiss Domes: Structure and metamorphic studies in Mabja Dome, southern Tibet: Journal of Structural Geology, v. 26, p. 2297–2316, doi:10.1016/j.jsg.2004.02.013.

Negredo, A.M., Replumaz, A., Villaseñor, A., and Guillot, S., 2007, Modeling the evolution of continental subduction processes in the Pamir–Hindu Kush region: Earth and Planetary Science Letters, v. 259, p. 212–225, doi:10.1016/j.epsl.2007.04.043.

Nelson, K.D., and 27 others, 1996, Partially molten middle crust beneath southern Tibet: Synthesis of project INDEPTH results: Science, v. 274, p. 1684–1688, doi:10.1126/science.274.5293.1684.

Quigley, M., Liangjun, Y., Wilson, C.J.L., Sandiford, M., and Phillips, D., 2006, $^{40}Ar/^{39}Ar$ thermochronology of the Kampa Dome, southern Tibet: Implications for tectonic evolution of the north Himalayan gneiss domes: Tectonophysics, v. 421, p. 269–297, doi:10.1016/j.tecto.2006.05.002.

Replumaz, A., Negredo, A.M., Guillot, S., and Villaseñor, A., 2010, Multiple episodes of continental subduction during India/Asia convergence: Insight from seismic tomography and tectonic reconstruction: Tectonophysics, v. 483, p. 125–134, doi:10.1016/j.tecto.2009.10.007.

Schmidt, J., Hacker, B.R., Ratschbacher, L., Stübner, K., Stearns, M., Kylander-Clark, A., Cottle, J.M., Alexander, A., Webb, G., Gehrels, G., and Minaev, V., 2011, Cenozoic deep crust in the Pamir: Earth and Planetary Science Letters, v. 312, p. 411–421, doi:10.1016/j.epsl.2011.10.034.

Schwab, M., Ratschbacher, L., Siebel, W., McWilliams, M., Minaev, V., Lutkov, V., Chen, F., Stanek, K., Nelson, B., Frisch, W., and Wooden, J.L., 2004, Assembly of the Pamirs: Age and origin of magmatic belts from the southern Tien Shan to the southern Pamirs and their relation to Tibet: Tectonics, v. 23, TC4002, doi:10.1029/2003TC001583.

Shannon, R.D., 1976, Revised effective ionic radii and systematic studies of interatomic distances in halides and chalcogenides: Acta Crystallographica, v. A32, p. 751–767.

Simpson, R.L., Parrish, R.R., Searle, M.P., and Waters, D.J., 2000, Two episodes of monazite crystallization during metamorphism and crustal melting in the Everest region of the Nepalese Himalaya: Geology, v. 28, p. 403–406, doi:10.1130/0091-7613(2000)28<403:TEOMCD>2.0.CO;2.

Streule, M.J., Searle, M.P., Waters, D.J., and Horstwood, M.S.A., 2010, Metamorphism, melting, and channel flow in the Greater Himalayan Sequence and Makalu leucogranites: Constraints form thermobarometry, metamorphic modeling, and U-Pb geochronology: Tectonics, v. 29, TC5011, doi:10.1029/2009TC002533.

van Hinsbergen, D.J.J., Steinberger, B., Doubrovine, P.V., and Gassmöller, R., 2011, Acceleration and deceleration of India-Asia convergence since the Cretaceous: Roles of mantle plumes and continental collision: Journal of Geophysical Research, v. 116, B06101, doi:10.1029/2010JB008051.

Williams, M.L., Jercinovic, M.J., and Terry, M.P., 1999, Age mapping and dating of monazite on the electron microprobe: Deconvoluting multistage tectonic histories: Geology, v. 27, p. 1023–1026, doi:10.1130/0091-7613(1999)027<1023:AMADOM>2.3.CO;2.

Manuscript received 4 February 2013
Revised manuscript received 27 May 2013
Manuscript accepted 30 May 2013

Printed in USA